

On what dynamic contrast-enhanced ultrasound tells us about the underlying vascular architecture

Citation for published version (APA):

Panfilova, A., Shelton, S. E., Caresio, C., van Sloun, R. J. G., Molinari, F., Wijkstra, H., Dayton, P. A., & Mischi, M. (2018). *On what dynamic contrast-enhanced ultrasound tells us about the underlying vascular architecture*. 7-11. Paper presented at 23rd European symposium on Ultrasound Contrast Imaging, January 18-19, 2018, Rotterdam, The Netherlands, Rotterdam, Netherlands.

Document status and date:

Published: 18/01/2018

Document Version:

Accepted manuscript including changes made at the peer-review stage

Please check the document version of this publication:

- A submitted manuscript is the version of the article upon submission and before peer-review. There can be important differences between the submitted version and the official published version of record. People interested in the research are advised to contact the author for the final version of the publication, or visit the DOI to the publisher's website.
- The final author version and the galley proof are versions of the publication after peer review.
- The final published version features the final layout of the paper including the volume, issue and page numbers.

[Link to publication](#)

General rights

Copyright and moral rights for the publications made accessible in the public portal are retained by the authors and/or other copyright owners and it is a condition of accessing publications that users recognise and abide by the legal requirements associated with these rights.

- Users may download and print one copy of any publication from the public portal for the purpose of private study or research.
- You may not further distribute the material or use it for any profit-making activity or commercial gain
- You may freely distribute the URL identifying the publication in the public portal.

If the publication is distributed under the terms of Article 25fa of the Dutch Copyright Act, indicated by the "Taverne" license above, please follow below link for the End User Agreement:

www.tue.nl/taverne

Take down policy

If you believe that this document breaches copyright please contact us at:

openaccess@tue.nl

providing details and we will investigate your claim.

On what dynamic contrast-enhanced ultrasound tells us about the underlying vascular architecture.

Anastasiia Panfilova¹, Sarah E. Shelton², Cristina Caresio³, Ruud J.G. van Sloun¹, Filippo Molinari³, Hessel Wijkstra^{1,4}, Paul A. Dayton², Massimo Mischi¹

¹Eindhoven University of Technology, Department of Electrical Engineering, Eindhoven, the Netherlands

²University of North Carolina at Chapel Hill and North Carolina State University, Joint Department of Biomedical Engineering, United States

³Politecnico di Torino, Department of Biomedical Engineering, Torino, Italy

⁴Academic Medical Center, University of Amsterdam, Department of Urology, Amsterdam, the Netherlands

Introduction

Cancer vascular morphology differs from that of healthy tissue [1]. These differences influence the tumor's blood flow dynamics, making dynamic contrast-enhanced ultrasound (DCE-US) a useful technique for cancer diagnostics. By quantitative DCE-US, time intensity curves (TICs) measured at each pixel are typically linearized to represent the time evolution of the ultrasound-contrast-agent (UCA) concentration. The shape of the resulting curves, referred to as indicator dilution curves (IDCs), has been shown useful for cancer diagnostics and is considered to reflect morphological properties of the underlying vascular system [2], [3].

DCE-US can be used for quantification of tissue perfusion, which is expected to increase in cancer lesions due to angiogenic hypervascularization. However, clinical research has demonstrated that perfusion alone is insufficient for an accurate diagnosis: cancer lesions can be iso- or hypo-perfused [4] as well as benign lesions can be hyper-perfused (e.g., fibro adenoma, [5]). A more recent approach quantifies the dispersion of UCAs flowing through the multipath trajectories provided by the numerous branches of the vascular network [6]. To this end, the shape similarity (correlation coefficient) between neighboring IDCs is estimated as an indicator of dispersion. This approach demonstrated its value for prostate cancer diagnostics in several preliminary clinical studies [6], [7]. However, its validation was mainly based on a comparison with histological measures of cell differentiation, disregarding the analysis of vascular features [8].

Characterization of the vasculature can be performed with acoustic angiography (AA), a high-resolution US technique that enables delineation of vessels as small as 100-200 micrometers in diameter [1], [9]. It utilizes a dual frequency transducer, transmitting at 4 MHz, close to the UCA bubble resonance frequency, and receiving the nonlinear UCA signal with a bandwidth centered at 30 MHz. The visualized vasculature can be segmented and characterized for its geometric properties.

The aim of this work is to determine which features of the vascular architecture are reflected in the standard perfusion and dispersion parameters, namely, the wash-in-rate (WIR) and the correlation coefficient between neighboring IDCs. To this end, DCE-US and AA imaging was executed on 9 rats implanted with a fibrosarcoma. Imaging was performed every 3 days, at 4 time points in total, monitoring the longitudinal evolution of the tumors. We sought for similar longitudinal trends. Moreover, a comparison of the spatial distribution of DCE-US and AA parameters was also performed for several cases.

Methods

Fibrosarcoma tumor models (Fischer 344 rats) were established from propagated tumor tissue implanted subcutaneously on the left flank of 9 rats. When the tumors were palpable, DCE-US and AA acquisitions of the tumor-bearing flank were performed while the animals were anesthetized with vaporized isoflurane in oxygen.

DCE-US imaging was executed with a Siemens Sequoia US scanner and a 15L8-A probe used in Contrast Pulse Sequencing mode at 7 MHz, following a UCA bolus injection (2×10^8 microbubbles). 3D AA images were acquired with a dual-frequency transducer, insonifying at 4 MHz and receiving at 30 MHz. A continuous infusion of UCA was administered using a syringe pump (PHD 2000, Harvard Apparatus) at a rate of 1.5×10^8 microbubbles per minute.

DCE-US dispersion maps were obtained by computing for each pixel the average correlation coefficient between the measured IDC and the IDCs extracted for the surrounding pixels over a ring with inner radius of 0.6 mm and outer radius of 2 mm. Assessment of DCE-US perfusion was performed by estimation of the UCA WIR, computed as the slope of a line fitted to the IDC in a 2-s interval after the appearance time, before the IDC peak.

Visible vessels were manually segmented in the AA volume, and their vessel radius (VR) and the sum of angles tortuosity metric (SOAM) were calculated [10]. The microvascular density (MVD) was calculated as the number of visible vessels per cm^3 . Values extracted from the tumor regions were assigned to the malignant group, while the surrounding region served as control.

A longitudinal study of the tumor evolution was performed by binning together parameter values for rats from the same time point. The same procedure was performed for the control.

It was noticed in this study that the WIR maps highlight large vessels, clearly visible in the AA volumes (indicated by arrows in Fig.1). When present in the DCE-US plane, these vessels were used as markers to identify the DCE-US plane in the AA volume. The identified corresponding slice (~ 1 mm thickness) in the AA volume was then processed with an extension of the skeletonization algorithm in [11]. This facilitated a qualitative comparison of the spatial distributions of the VR, SOAM, and MVD with those of perfusion and dispersion in the same plane.

All experiments were approved by the Institutional Animal Care and Use Committee at the University of North Carolina at Chapel Hill.

Results

The longitudinal analysis shows a relatively stable dispersion for control and tumor, with significantly higher values in tumor (Fig. 1 a.). Perfusion peaks for the young tumors at the second time point, and declines as the tumor develops, remaining higher in tumor compared to control (Fig. 1 b.). The MVD shows a similar trend as perfusion (Fig. 1 b. and c.). Areas with high perfusion, besides large vessels (shown by arrows in the AA in Fig 2. a. and perfusion images in Fig. 2 e.), correspond to areas with high MVD (Fig. 2).

Dispersion and the SOAM have a similar longitudinal trend (Fig. 1 d.). However, different from dispersion, the difference between the SOAM for control and tumor is small. We were not able to find an agreement between the spatial distribution of dispersion and the characteristics extracted from the AA slices (Fig. 2).

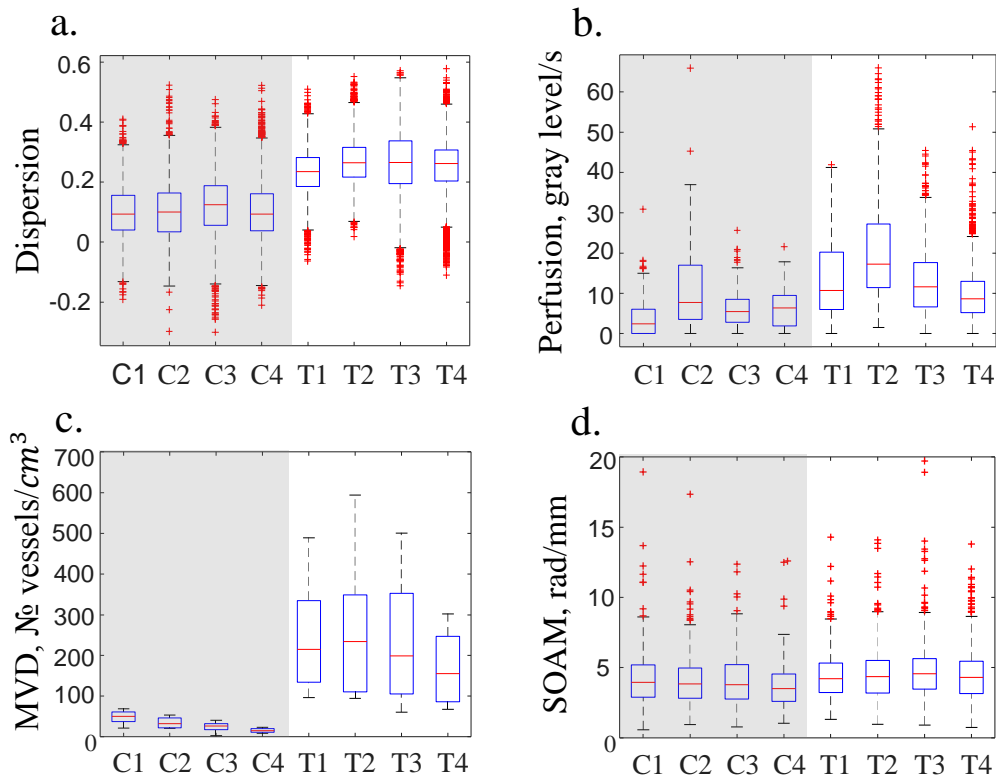


Fig. 1. Longitudinal trends. a-b: DCE-US dispersion and perfusion; c-d: microvascular density and sum of angles metric extracted from AA. Control evolution at time points 1 to 4 (C1, C2, C3, C4) is shown on a gray background. Tumor evolution is on a white background (T1, T2, T3, T4).

Conclusions and Discussion

The parametric maps of dispersion and perfusion seem complementary (Fig. 2), highlighting different regions of the tumor. No agreement could be found between dispersion and the extracted AA features. Instead, the performed analysis indicates perfusion and MVD to be better correlated. Yet, we should consider that the MVD extracted in this work is limited to vessels larger than 100-200 micrometers in diameter. Interestingly, dispersion provided the best tumor classification, also compared to AA parameters. Altogether, we may conclude that important microvascular features relate to smaller vessels, which could not be investigated by AA. Indeed, additional studies are required to investigate the relationship between smaller vessels with the corresponding perfusion and dispersion maps. Such studies may elucidate the relation between cancer angiogenic processes and the estimated perfusion and dispersion maps.

Acknowledgement

This work was supported by the European Research Council Starting Grant (#280209) and the Impulse2 program within TU/e and Philips.

This work was also supported by R01CA170665, R43CA165621, R01CA189479, and F99CA212227 from the National Institutes of Health. Paul Dayton is an inventor on a patent describing acoustic angiography and a co-founder of a company which has licensed this technology.

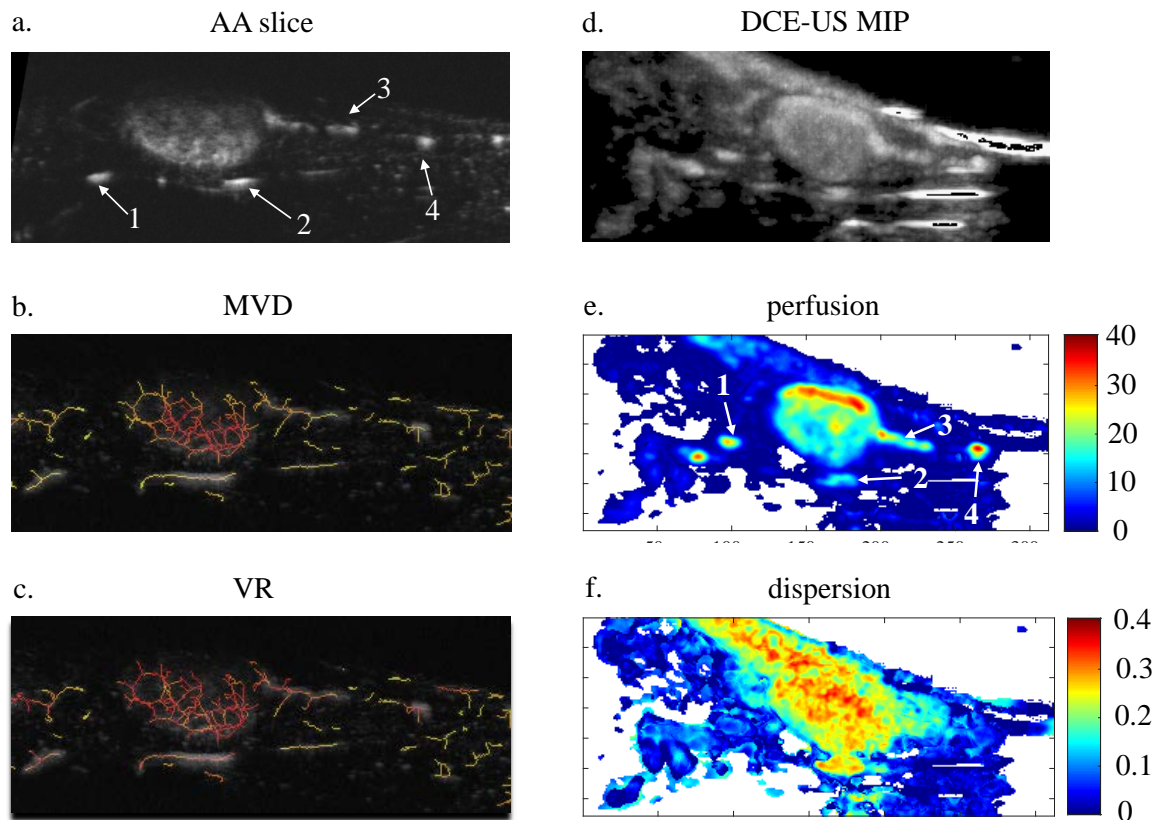


Fig. 2. Maps illustrating the spatial distribution of the DCE-US and AA parameters. a: AA image reconstructed from 25 slices (~ 1 mm thickness); b-c: vascular skeleton with the color-coded microvascular density and mean vessel radius, respectively (red indicating high values and yellow - low values). d: DCE-US maximum intensity projection with the black regions corresponding to low intensity regions. e-f: maps of perfusion and dispersion, respectively, with white regions corresponding to low intensity regions, excluded from the analysis. The numbers in the figures point to the large vessel structures that were used to register the DCE-US plane in the AA volume.

- [1] S. E. Shelton *et al.*, "Quantification of microvascular tortuosity during tumor evolution using acoustic angiography," *Ultrasound Med. Biol.*, vol. 41, no. 7, pp. 1896–1904, 2015.
- [2] M. P. J. Kuenen, M. Mischi, and H. Wijkstra, "Contrast-ultrasound diffusion imaging for localization of prostate cancer," *IEEE Trans. Med. Imaging*, vol. 30, no. 8, pp. 1493–1502, 2011.
- [3] M. P. J. Kuenen, T. A. Saidov, H. Wijkstra, and M. Mischi, "Contrast-Ultrasound Dispersion Imaging for Prostate Cancer Localization by Improved Spatiotemporal Similarity Analysis," *Ultrasound Med. Biol.*, vol. 39, no. 9, pp. 1631–1641, 2013.
- [4] M. Brock *et al.*, "Multiparametric ultrasound of the prostate: adding contrast enhanced ultrasound to real-time elastography to detect histopathologically confirmed cancer.," *J. Urol.*, vol. 189, no. 1, pp. 93–8, 2013.
- [5] E. M. Jung *et al.*, "Contrast enhanced harmonic ultrasound for differentiating breast tumors - first results.," *Clin. Hemorheol. Microcirc.*, vol. 33, no. 2, pp. 109–120, 2005.
- [6] M. Mischi, M. P. J. Kuenen, and H. Wijkstra, "Angiogenesis imaging by spatiotemporal analysis of ultrasound contrast agent dispersion kinetics," *IEEE Trans. Ultrason. Ferroelectr. Freq. Control*, vol. 59, no. 4, pp. 621–629, 2012.

- [7] M. P. J. Kuenen, T. A. Saidov, H. Wijkstra, J. J. M. C. H. De La Rosette, and M. Mischi, "Spatiotemporal correlation of ultrasound contrast agent dilution curves for angiogenesis localization by dispersion imaging," *IEEE Trans. Ultrason. Ferroelectr. Freq. Control*, vol. 60, no. 12, pp. 2665–2669, 2013.
- [8] M. Mischi, C. Heneweer, J. Von Broich-Oppert, T. Saidov, and H. Wijkstra, "Fractal dimension of tumor microvasculature by dynamic contrast-enhanced ultrasound," in *2015 IEEE International Ultrasonics Symposium, IUS 2015*, 2015.
- [9] R. C. Gessner, C. B. Frederick, F. S. Foster, and P. A. Dayton, "Acoustic angiography: A new imaging modality for assessing microvasculature architecture," *Int. J. Biomed. Imaging*, vol. 2013, 2013.
- [10] E. Bullitt, G. Gerig, S. M. Pizer, W. Lin, and S. R. Aylward, "Measuring Tortuosity of the Intracerebral Vasculature from MRA Images," *IEEE Trans. Med. Imaging*, vol. 22, no. 9, pp. 1163–1171, 2003.
- [11] K. M. Meiburger, S. Y. Nam, E. Chung, L. J. Suggs, S. Y. Emelianov, and F. Molinari, "Skeletonization algorithm-based blood vessel quantification using in vivo 3D photoacoustic imaging," *Phys. Med. Biol.*, vol. 61, no. 22, pp. 7994–8009, 2016.